Linear Algebra and its Applications 545 (2018) 148–173

Contents lists available at ScienceDirect

Linear Algebra and its Applications

www.elsevier.com/locate/laa

Classification of joint numerical ranges of three hermitian matrices of size three

Konrad Szymański [a], Stephan Weis [b,*], Karol Życzkowski [a,c]

[a] *Marian Smoluchowski Institute of Physics, Jagiellonian University, Łojasiewicza 11, 30-348 Kraków, Poland*
[b] *Centre for Quantum Information and Communication, Université libre de Bruxelles, 50 av. F.D. Roosevelt – CP165/59, 1050 Bruxelles, Belgium*
[c] *Center for Theoretical Physics of the Polish Academy of Sciences, Al. Lotnikow 32/46, 02-668 Warsaw, Poland*

A R T I C L E   I N F O

Article history:
Received 29 March 2016
Accepted 20 November 2017
Available online 24 November 2017
Submitted by C.-K. Li

MSC:
47A12
47L07
52A20
52A15
52B05
05C10

Keywords:
Joint numerical range
Density matrices
Exposed face
Generic shape
Classification

A B S T R A C T

The joint numerical range $W(F)$ of three hermitian 3-by-3 matrices $F = (F_1, F_2, F_3)$ is a convex and compact subset in $\mathbb{R}^3$. Generically we find that $W(F)$ is a three-dimensional oval. Assuming $\dim(W(F)) = 3$, every one- or two-dimensional face of $W(F)$ is a segment or a filled ellipse. We prove that only ten configurations of these segments and ellipses are possible. We identify a triple F for each class and illustrate $W(F)$ using random matrices and dual varieties.

* Corresponding author.
E-mail addresses: konrad.szymanski@uj.edu.pl (K. Szymański), maths@weis-stephan.de (S. Weis), karol.zyczkowski@uj.edu.pl (K. Życzkowski).

https://doi.org/10.1016/j.laa.2017.11.017
0024-3795/© 2017 Published by Elsevier Inc.

1. Introduction

We denote the space of complex d-by-d matrices by M_d, $d \in \mathbb{N}$, $\mathbb{N} = \{1, 2, 3, \ldots\}$. We write $M_d^{\mathrm{h}} := \{a \in M_d \mid a^* = a\}$ for the real subspace of hermitian matrices and $\mathbb{1}_d \in M_d$ for the identity matrix. We write $\langle x, y\rangle := \overline{x_1}y_1 + \cdots + \overline{x_d}y_d$, $x, y \in \mathbb{C}^d$ for the inner product on $\mathbb{C}^d$. Let $F := (F_1, \ldots, F_n) \in (M_d^{\mathrm{h}})^n$, $n \in \mathbb{N}$. The *joint numerical range* of F is

$$W(F) := \{(\langle x, F_1x\rangle, \ldots, \langle x, F_nx\rangle) \mid x \in \mathbb{C}^d, \langle x, x\rangle = 1\} \subset \mathbb{R}^n.$$

For $n = 2$, when identifying $\mathbb{R}^2 \cong \mathbb{C}$, the set $W(F_1, F_2)$ is known as the *numerical range* $\{\langle x, Ax\rangle \mid x \in \mathbb{C}^d, \langle x, x\rangle = 1\}$ of the matrix $A := F_1 + \mathrm{i}\, F_2$. The numerical range is convex by the Toeplitz–Hausdorff theorem [55,28]. Similarly, for $n = 3$ and all $d \geq 3$ the joint numerical range $W(F_1, F_2, F_3)$ is convex [2]. However, $W(F)$ is in general not convex for $n \geq 4$, see [45,41,25].

The shape of the numerical range ($n = 2$) is well understood. The elliptical range theorem [40] states that if $d = 2$, then $W(F_1, F_2)$ is a singleton, segment, or filled ellipse. Kippenhahn [35] proved for all $d \in \mathbb{N}$ that the numerical range is the convex hull of the boundary generating curve defined in Remark 1.2. To explain the resulting classification of $W(F_1, F_2)$ for $d = 3$ let first d, n be arbitrary. We say that F is *unitarily reducible* if there is a unitary $U \in M_d$ such that the matrices $U^*F_1U, \ldots, U^*F_nU$ have a common block diagonal form with two proper blocks. Otherwise F is *unitarily irreducible*. Let $d = 3$ and $n = 2$. If $F = (F_1, F_2)$ is unitarily reducible, then the numerical range $W(F_1, F_2)$ is a singleton, segment, triangle, ellipse, or the convex hull of an ellipse and a point outside the ellipse. If F is unitarily irreducible, then $W(F)$ is an ellipse, the convex hull of a quartic curve (with a flat portion on the boundary), or the convex hull of a sextic curve (an oval). These classes were also characterized in terms of matrix invariants and entries of $F_1 + \mathrm{i}\, F_2$, see [34,49,47,54]. The boundary generating curve also yields a classification of numerical ranges of 4-by-4 matrices [16]. Another result [30,29] is that a subset W of $\mathbb{C}$ is the numerical range of some d-by-d matrix if and only if it is a translation of the polar of a rigidly convex set of degree less than or equal to d, see Corollary 3 of [29]. We omit the details of this last description as we will not use it.

Despite a long history of the problem [8,36,14,15,12], a classification of the joint numerical range was unknown for $n = 3$ even in the simple case of $d = n = 3$. Our motivation to study this problem is quantum mechanics, as we explain in Section 2. The link to physics is that for arbitrary $d, n \in \mathbb{N}$ the convex hull $\mathrm{conv}(W(F))$ of the joint numerical range is a projection (image under a linear map) of the state space $\mathcal{M}_d$ of the algebra M_d [19]. The latter consists of d-by-d *density matrices*, that is positive semi-definite matrices of trace one, which represent states of quantum systems. To study the joint numerical range $W(F)$ for $d = n = 3$ (where $W(F)$ is convex), one of us computed exemplary joint numerical ranges from random matrices [59]. Some printouts from a 3D-printer are shown in Fig. 1. The object in Fig. 1f) served as a starting point for this research.

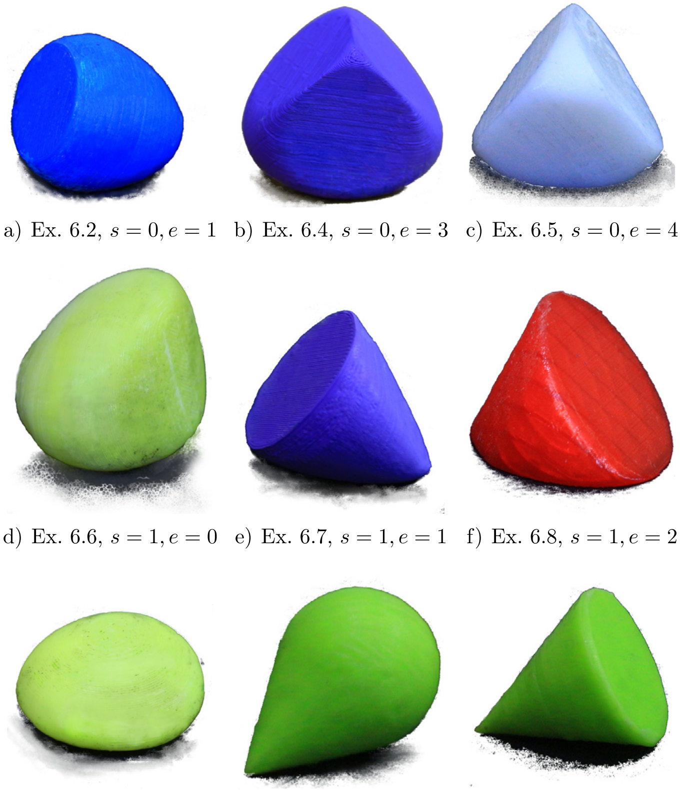

a) Ex. 6.2, $s = 0, e = 1$ b) Ex. 6.4, $s = 0, e = 3$ c) Ex. 6.5, $s = 0, e = 4$

d) Ex. 6.6, $s = 1, e = 0$ e) Ex. 6.7, $s = 1, e = 1$ f) Ex. 6.8, $s = 1, e = 2$

g) $s = e = 0$ h) $s = \infty, e = 0$ i) $s = \infty, e = 1$

Fig. 1. 3D printouts of exemplary joint numerical ranges of triples of hermitian 3-by-3 matrices from random density matrices: s denotes the number of segments, e the number of ellipses in the boundary.

We present a simple classification of $W(F)$ for $d = n = 3$ in terms of *exposed faces* of $W(F)$. An exposed face is a subset of $W(F)$ which is either empty or consists of the maximizers of a linear functionals on $W(F)$. Let $d = n = 3$. Then $W(F)$ is convex and Lemma 4.3 shows that the non-empty exposed faces of $W(F)$ which are neither singletons nor equal to $W(F)$ are segments or filled ellipses. We call them *large faces* of $W(F)$ and collect them in the set

$$\begin{aligned}\mathcal{L}(F) := \{&G \text{ is an exposed face of } W(F) \mid \\ &G \neq W(F) \text{ and } G \text{ is a segment or a filled ellipse}\}.\end{aligned} \tag{1.1}$$

Throughout the introduction, let e (resp. s) denote the number of filled ellipses (resp. segments) in $\mathcal{L}(F)$. We recall that a *corner point* of $W(F)$ is a point which lies on three supporting hyperplanes with linearly independent normal vectors.

Theorem 1.1. *Let $F \in (M_3^{\mathrm{h}})^3$. If $W(F)$ has no corner point, then the set $\mathcal{L}(F)$ of large faces of $W(F)$ has one of the eight configurations of Fig. 2.*

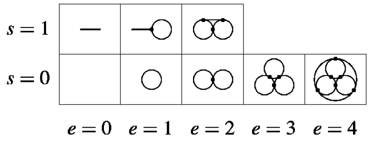

Fig. 2. Configurations of the set $\mathcal{L}(F)$ of large faces of the joint numerical range $W(F)$ for three hermitian 3-by-3 matrices $F = (F_1, F_2, F_3)$ assuming that $W(F)$ has no corner point. Circles (resp. segments) denote large faces which are filled ellipses (resp. segments). Dots denote intersection points between large faces.

Proof. It is easy to see that large faces intersect mutually (Lemma 5.1). Since $W(F)$ has no corner point, no point lies on three mutually distinct large faces (Lemma 5.2). Hence the union of large faces contains an embedded complete graph with one vertex on each large face (Lemma 5.3). Now, a well-known theorem of graph embedding [48] shows $e + s \leq 4$. Next we observe that $s = 0, 1$ holds, because otherwise $W(F)$ has a corner point (Lemma 5.4). Finally, we exclude the case $(e, s) = (3, 1)$ by observing that for $s = 1$ the embedded graph has a vertex on a segment and hence it has vertex degree at most two. □

For each of the eight configurations of Fig. 2 Section 6 presents an example of a joint numerical range $W(F)$ for $F \in (M_3^{\mathrm{h}})^3$ such that $W(F)$ has dimension three and no corner points. To the best of our knowledge, the configurations

$$(e, s) \quad = \quad (1, 0), \quad (2, 0), \quad (3, 0), \quad \text{or} \quad (0, 1)$$

were unknown prior to this work. Ovals, where $(e, s) = (0, 0)$, were studied in [36]. An example of $(e, s) = (4, 0)$ can be found in [31], one of $(e, s) = (1, 1)$ in [15], and one of $(e, s) = (2, 1)$ in [9].

Concerning corner points, if $W(F)$ has some of them and if $\dim(W(F)) = 3$, then $(e, s) = (0, \infty)$ or $(e, s) = (1, \infty)$ holds by Lemma 4.9. In the former case $W(F)$ is the convex hull of an ellipsoid and a point outside the ellipsoid. In the latter case $W(F)$ is the convex hull of an ellipse and a point outside the affine hull of the ellipse. Examples are depicted in Fig. 1h) and 1i).

If $\dim(W(F)) = 2$ then we have $e = 0$. By projecting to a plane, $W(F)$ corresponds to the numerical range of a 3-by-3 matrix. Notice that $W(F)$ belongs to one of four classes of 2D objects characterized by the number of segments $s = 0, 1, 2, 3$. The classification of $W(F)$ in terms of large faces is courser than the classification [35] explained above.

Remark 1.2. Let $F \in (M_3^{\mathrm{h}})^3$.

(1) Any joint numerical range $W(F)$ of dimension three which has a large face G of the form of a segment ($s = 1$) answers a question of [57] (examples were already given in [9,50]). Namely, a limit of extreme points of $\mathcal{M}_d$, $d \in \mathbb{N}$, is again an extreme point. The question was whether the analogue holds for projections of $\mathcal{M}_d$. This doubt is dispelled by observing that any point in the relative interior of G is a limit of extreme

points but not an extreme point itself. A simpler example with 4-by-4 matrices is the skew cone $W(F_1, F_2, F_3)$ for

$$F_1 = \begin{pmatrix} 1 & 0 & 0 & 0 \\ 0 & -1 & 0 & 0 \\ 0 & 0 & 1 & 0 \\ 0 & 0 & 0 & 1 \end{pmatrix}, \qquad F_2 = \begin{pmatrix} 0 & 1 & 0 & 0 \\ 1 & 0 & 0 & 0 \\ 0 & 0 & 0 & 0 \\ 0 & 0 & 0 & 0 \end{pmatrix}, \qquad F_3 = \begin{pmatrix} 0 & 0 & 0 & 0 \\ 0 & 0 & 0 & 0 \\ 0 & 0 & -1 & 0 \\ 0 & 0 & 0 & 1 \end{pmatrix},$$

which is the convex hull of the union of the unit disk in the x-y-plane with the points $(1, 0, \pm 1)$.

(2) For arbitrary $d, n \in \mathbb{N}$ we consider the hypersurface in the complex projective space $\mathbb{P}^n$, defined as the zero locus

$$S_F := \{(u_0 : \cdots : u_n) \in \mathbb{P}^n \mid \det(u_0 \mathbb{1} + u_1 F_1 + \cdots + u_n F_n) = 0\}$$

of a determinant. An analysis of singularities of S_F for $d = n = 3$ shows that the joint numerical range $W(F)$ has at most four large faces which are ellipses [14]. This estimate also follows from our classification. In Section 6 we use algebraic geometry for a heuristic drawing method of $W(F)$. The *dual variety* $S_F^* \subset \mathbb{P}^{n*}$ of S_F is the complex projective variety which is the closure of the set of tangent hyperplanes of S_F at smooth points [22,27,24]. The *boundary generating hypersurface* [15] of F is defined to be the real affine part of the dual variety S_F^*,

$$S_F^*(\mathbb{R}) = \{(x_1, \ldots, x_n) \in \mathbb{R}^n \mid (1 : x_1 : \cdots : x_n) \in S_F^*\}.$$

For $n = 2$ the variety $S_F^*(\mathbb{R})$ is called *boundary generating curve* and Kippenhahn [35] showed that its convex hull is the numerical range, see also [15]. For $d = n = 3$, Chien and Nakazato [15] discovered that the surface $S_F^*(\mathbb{R})$ can contain (unbounded) lines, so the analogue of the Kippenhahn assertion for $n \geq 3$ does not hold. We will see examples of such lines in Section 6.

The generic joint numerical range of three hermitian 3-by-3 matrices is an *oval*, that is a compact convex set with interior points, which is strictly convex and has a smooth boundary. More precisely, we point out in Theorem 4.2 that $W(F)$ is generically an oval for $d \geq 2$ and $n \leq 3$ (in the exceptional case $d = 2, n = 3$ the joint numerical range $W(F)$ is generically a hollow ellipsoid, but $\text{conv}(W(F))$ is an oval). This result follows from the von Neumann–Wigner *non-crossing rule* [44,25] and from a study of normal cones in Section 3. Conversely, using the *crossing rule* [23] we show in Lemma 4.6 that no join numerical range $W(F)$ is an oval for $d = 3$, $n \geq 6$. For real symmetric matrices F, ovals are generic for $d \geq 2$ and $n \leq 2$, but do not appear for $d = 3$ and $n \geq 4$. Section 4 also collects other methods to study exposed faces, such as spectral representation, discriminants, sum of squares decompositions, and corner points.

Acknowledgments. SW thanks for discussions Didier Henrion, Konrad Schmüdgen, and Rainer Sinn. It is a pleasure to thank the “Complexity Garage” at the Jagiellonian

University, where all the 3D printouts were made, and to Lia Pugliese for taking their photos. We acknowledge support by a Brazilian CAPES scholarship (SW), by the Polish National Science Centre under the project number DEC-2011/02/A/ST1/00119 (KŻ) and by the project #56033 financed by the Templeton Foundation. Research was partially completed while SW was visiting the Institute for Mathematical Sciences, National University of Singapore in 2016.

2. Quantum states

Our interest in the joint numerical range is its role in quantum mechanics where the hermitian matrices M_d^{h} are called Hamiltonians or observables, see e.g. [7], and they correspond to physical systems with d energy levels or measurable quantities having d possible outcomes.

Usually a (complex) C*-subalgebra $\mathcal{A}$ of M_d is considered as the algebra of observables of a quantum system [1]. If $a \in M_d$ is positive semi-definite then we write $a \succeq 0$. The physical states of the quantum system are described by d-by-d density matrices which for the *state space* of $\mathcal{A}$,

$$\mathcal{M}(\mathcal{A}) := \{\rho \in \mathcal{A} \mid \rho \succeq 0, \mathrm{tr}(\rho) = 1\}. \tag{2.1}$$

It is well-known that $\mathcal{M}(\mathcal{A})$ is a compact convex subset of M_d^{h}, see for example Theorem 4.6 of [1]. We use the inner product $\langle a, b\rangle := \mathrm{tr}(a^* b)$, $a, b \in M_d$. We are mainly interested in $\mathcal{M}_d := \mathcal{M}(M_d)$ but in Sec. 4 also in the compressed algebra $pM_d p$ where $p \in M_d$ is an orthogonal projection operator, that is $p^2 = p^* = p$. The state space $\mathcal{M}(pM_d p)$ is, as we recall in Sec. 4, an exposed face of $\mathcal{M}_d$, see [1,56]. The state space $\mathcal{M}_2$ is a Euclidean ball, called *Bloch ball*, but $\mathcal{M}_d$ is not a ball [7] for $d \geq 3$. Although several attempts were made to analyze properties of this set [33,6,52,37,38], its complicated structure requires further studies.

If the quantum system is in the state $\rho \in \mathcal{M}_d$, then the expected value of a Hamiltonian $a \in M_d$, is the real number $\langle \rho, a\rangle$. Thus the standard numerical range $W(F_1, F_2)$ of a non-hermitian operator $A = F_1 + iF_2$ can be considered as the set of all expectation values of possible outcomes of measurements of two hermitian operators F_1 and F_2 performed on two copies of the same quantum state ρ. Furthermore, this set can be identified [19,46] as a projection of the set $\mathcal{M}_d$ of quantum states onto a two-plane. The Dvoretzky theorem [20] implies that for large dimension d a generic 2D projection of the convex set $\mathcal{M}_d$ is close to a circular disk, so that the numerical range $W(A)$ of a non-hermitian random matrix A of the Ginibre ensemble typically forms a disk [17].

In this work we analyze the joint numerical range of a triple of hermitian matrices of size three. As in the case of a pair of matrices, they can be interpreted as sets of expectation values of possible results of measurements of three hermitian observables performed on three copies of the same quantum state. On the other hand they form projections of the 8D set of density matrices of size three into $\mathbb{R}^3$, see [26]. A special case for larger matrix dimensions are projections to subsystems, whose geometry was recently studied [58,10,11] to investigate the structure of reduced density matrices for many-body quantum systems.

Consider a general case, $d, n \in \mathbb{N}$, of the joint numerical range of n hermitian matrices $F = (F_1, \dots, F_n) \in (M_d^{\mathrm{h}})^n$ of size d. In this paper we will use the linear map

$$\mathbb{E}_F : M_d^{\mathrm{h}} \to \mathbb{R}^n, \quad a \mapsto (\langle a, F_1 \rangle, \dots, \langle a, F_n \rangle)$$

to study the image

$$L(F) := \mathbb{E}_F(\mathcal{M}_d) = \{\mathbb{E}_F(\rho) \mid \rho \in \mathcal{M}_d\} \subset \mathbb{R}^n \tag{2.2}$$

of the state space $\mathcal{M}_d = \mathcal{M}(M_d)$ defined in (2.1). The set $L(F)$ is known as the *joint algebraic numerical range* [43]. We call $L(F)$ *convex support* [56], which for commutative matrices is its name in statistics [4]. The convex support is a compact convex subset of $\mathbb{R}^n$ and equals the convex hull of the joint numerical range

$$L(F) = \mathrm{conv}(W(F)). \tag{2.3}$$

A proof of equation (2.3) is given in [43] by reduction of $n \in \mathbb{N}$ to the case $n = 2$. The proof given in [26] uses linear algebra. We recall that for $n = 3$ and $d \geq 3$ we have $L(F) = W(F)$ because $W(F)$ is convex. In what follows, we will work with $L(F)$ rather than $W(F)$.

Some of the 3-D images are generated using random sampling – this method is simple conceptually and produces objects which are accurate enough for use in printing. In this numerical procedure, which we implemented in Mathematica, we calculate a finite number (of order of 10^5) of points inside $W(F)$,

$$\{(\langle x, F_1 x \rangle, \dots, \langle x, F_n x \rangle) \mid x \in S\},$$

where S is the set of points sampled from the uniform distribution on a complex $(d-1)$-dimensional sphere (this step is realized by sampling points from complex d-dimensional Gaussian distribution and normalizing the result). A convex hull of generated points is then calculated using `ConvexHullMesh` procedure and exported to an `.stl` file, which contains a description of the 3-D object recognized by the software used in printing. The final objects were made with PIRX One 3-D printer.

3. Normal cones and ovals

We show that convex support sets have in a sense many normal cones. Then we prove that this property allows to characterize ovals in terms of strict convexity.

A *face* of a convex subset $C \subset \mathbb{R}^m$, $m \in \mathbb{N}$, is a convex subset of C which contains the endpoints of every open segment in C which it intersects. An *exposed face* of C is defined as the set of maximizers of a linear functional on C. If C is non-empty and compact, then for every $u \in \mathbb{R}^m$ the set

$$\mathbb{F}_C(u) := \underset{x \in C}{\operatorname{argmax}} \langle x, u \rangle \tag{3.1}$$

is an exposed face of C. From now on, the empty set is defined to be an exposed face as well (then the set of exposed faces forms a lattice). It is well-known that every exposed face is a face. If a face (resp. exposed face) is singleton, then we call its element an *extreme point* (resp. *exposed point*). A face (resp. exposed face) of C which is different from $\emptyset, C$ is called *proper face* (resp. proper exposed face).

Let $C \subset \mathbb{R}^m$ be a convex subset and $x \in C$. The *normal cone* of C at x is

$$N(x) := \{u \in \mathbb{R}^m \mid \forall y \in C : \langle u, y - x \rangle \leq 0\}.$$

Elements of $N(x)$ are called *(outer) normal vectors* of C at x. It is well-known that there is a non-zero normal vector of C at x if and only if x is a boundary point of C. In that case x is *smooth* if C admits a unique outer unit normal vector at x.

The normal cone of C at a non-empty face G of C is well-defined as the normal cone $N(G) := N(x)$ of C at any point x in the relative interior of G (the relative interior of G is the interior of G with respect to the topology of the affine hull of G). See for example Section 4 of [57] about the consistency of this definition, and set $N(\emptyset) := \mathbb{R}^m$. The convex set C is a *convex cone* if $C \neq \emptyset$ and if $x \in C$, $\lambda \geq 0$ implies $\lambda x \in C$. A *ray* is a set of the form $\{\lambda \cdot u \mid \lambda \geq 0\} \subset \mathbb{R}^m$ for non-zero $u \in \mathbb{R}^m$. An *extreme ray* of C is a ray which is a face of C.

We denote the set of exposed faces and normal cones of C by $\mathcal{E}_C$ and $\mathcal{N}_C$, respectively. Each of these sets is a *lattice* partially ordered by inclusion, that is the infimum $x \wedge y$ and supremum $x \vee y$ exist for all x, y in the set. A *chain* in a lattice is a totally ordered subset, its *length* is its cardinality minus one. The *length* of a lattice is the supremum of the lengths of all its chains. Lattices of faces have been studied earlier [3,42], in particular these of state spaces [1], and linear images $L(F)$ of state spaces [56]. By Proposition 4.7 of [57], if C is not a singleton then

$$\mathcal{E}_C \to \mathcal{N}_C, \quad G \mapsto N(G) \tag{3.2}$$

is an antitone lattice isomorphism. This means that the map is a bijection and for all exposed faces G, H we have $G \subset H$ if and only if $N(G) \supset N(H)$.

What makes normal cones of a convex support set C special is that all their non-empty faces are normal cones of C, too, as we will see in Lemma 3.1. For two-dimensional $C \subset \mathbb{R}^2$ this means that a boundary point of C is smooth unless it is the intersection of two one-dimensional faces of C, as one can see from the isomorphism (3.2). That property is well-known [5] for the numerical range $W(A)$ of a matrix $A \in M_d$. For example, the half-moon $\{z \in \mathbb{C} : |z| \leq 1, \Re(z) \geq 0\}$ is not the numerical range of any matrix. That observation also follows from Anderson's theorem [13] which asserts that if $W(A)$ is included in the unit disk and contains $d+1$ distinct points of the unit circle, then $W(A)$ equals the unit disk.

To prove the lemma we introduce the Definitions 6.1 and 7.1 of [57] for the special case of a non-empty, compact, and convex subset $C \subset \mathbb{R}^m$. Let $u \in \mathbb{R}^m$ be a non-zero vector. Then u is called *sharp normal* for C if for every relative interior point x of the exposed face $\mathbb{F}_C(u)$ the vector u is a relative interior point of the normal cone of C at x. The *touching cone* of C at u is defined to be the face of the normal cone of C at $\mathbb{F}_C(u)$ which contains u in its relative interior. The linear space $\mathbb{R}^m$ and the orthogonal complement of the translation vector space of the affine hull of C are touching cones of C by definition. We point out that, by Lemma 7.2 of [57], every normal cone of C is a touching cone of C.

Lemma 3.1. *Every non-empty face of every normal cone of $L(F)$ is a normal cone of $L(F)$.*

Proof. Propositions 2.9 and 2.11 of [56] prove that every non-zero hermitian d-by-d matrix is sharp normal for the state space $\mathcal{M}_d$. Therefore, Proposition 7.6 of [57] shows that every touching cone of $\mathcal{M}_d$ is a normal cone of $\mathcal{M}_d$. Corollary 7.7 of [57] proves that $L(F)$, being a projection of $\mathcal{M}_d$, has the analogous property. The characterization of touching cones as the non-empty faces of normal cones, given in Theorem 7.4 of [57], completes the proof. □

We define an *oval* as a convex and compact subset of $\mathbb{R}^m$ with interior points each of whose boundary points is a smooth exposed point. Notice that by this definition ovals are strictly convex and smooth. For the following class of convex sets strict convexity implies smoothness.

Lemma 3.2. *Let $C \subset \mathbb{R}^m$ be a convex and compact subset of $\mathbb{R}^m$ with interior points, such that every extreme ray of every normal cone of C is a normal cone of C. Then C is an oval if and only if all proper exposed faces of C are singletons.*

Proof. We assume first that C is an oval. By definition, the boundary of C is covered by extreme points. Since C is the disjoint union of the relative interiors of its faces, see for example Theorem 2.1.2 of [53], this shows that all proper faces of C are singletons.

To prove the converse part we observe that, since C has full dimension, the proper faces of C cover the boundary ∂C. Since every proper face lies in a proper exposed face, see for example Lemma 4.6 of [57], it follows that ∂C is covered by exposed points. We finish the proof by showing that C is smooth. Let x be a boundary point of C. As $\dim(C) = m$, the normal cone $N(x)$ contains no line and so it has at least one extreme ray which we denoted by r (see e.g. Theorem 1.4.3 of [53]). By assumptions, r is a normal cone of C. So

$$\{0\} \subset r \subset N(x) \subset \mathbb{R}^m$$

is a chain in the lattice $\mathcal{N}_C$ of normal cones. Thereby the inclusions $\{0\} \subset r$ and $N(x) \subset \mathbb{R}^m$ are proper. Since all proper exposed faces of C are singletons, the lattice $\mathcal{E}_C$ of exposed faces has length two, hence the isomorphism (3.2) shows that $\mathcal{N}_C$ has length two. This proves $N(x) = r$, for otherwise the chain $\{0\} \subset r \subset N(x) \subset \mathbb{R}^m$ had length three. Therefore x has a unique outer unit normal vector. This completes the proof. □

4. Exposed faces

This section collects methods to study exposed faces of the convex support $L(F)$. We start with the well-known representation of exposed faces in terms of eigenspaces of the greatest eigenvalues of real linear combinations of $F_1, \ldots, F_n$. This allows us to show that the generic shape of $L(F)$ is an oval for $n = 1, 2, 3$ ($n = 1, 2$ for real symmetric F_i's). For 3-by-3 matrices we discuss the discriminant of the characteristic polynomial and the sum of squares decomposition of its modulus, which we use later to detect large faces. We further discuss pre-images of exposed points. This allows us to prove that $L(F)$ is no oval for $d = 3$ if $n \geq 6$ ($n \geq 4$ for real symmetric matrices). Finally we address corner points.

Let $d, n \in \mathbb{N}$ be arbitrary. As before we write $F = (F_1, \ldots, F_n) \in (M_d^{\mathrm{h}})^n$ and we define

$$F(u) := u_1 F_1 + \cdots + u_n F_n, \qquad u \in \mathbb{R}^n.$$

By (2.2) the convex support $L(F)$ is the image of the state space $\mathcal{M}_d$ under the map $\mathbb{E}_F$. So all subsets of $L(F)$ are equivalently described in terms of their pre-images under the restricted map $\mathbb{E}_F|_{\mathcal{M}_d}$. In particular, the exposed face $\mathbb{F}_{L(F)}(u)$ of $L(F)$, in the notation from (3.1), has the pre-image

$$\mathbb{E}_F|_{\mathcal{M}_d}^{-1}(\mathbb{F}_{L(F)}(u)) = \mathbb{F}_{\mathcal{M}_d}(F(u)) = \operatorname{argmax}_{\rho \in \mathcal{M}_d} \langle \rho, F(u) \rangle. \tag{4.1}$$

See for example Lemma 5.4 of [57] for this simple observation. The relation (4.1) offers an algebra access to exposed faces of $L(F)$. For $a \in M_d^{\mathrm{h}}$ the exposed face $\mathbb{F}_{\mathcal{M}_d}(a) = \mathcal{M}(pM_dp)$ of the state space $\mathcal{M}_d = \mathcal{M}(M_d)$ is the state space of the algebra pM_dp where p is the spectral projection of a corresponding to the greatest eigenvalue, see [1] or [56]. Therefore (4.1) shows

$$\mathbb{E}_F|_{\mathcal{M}_d}^{-1}(\mathbb{F}_{L(F)}(u)) = \mathcal{M}(pM_dp), \qquad u \in \mathbb{R}^n, \tag{4.2}$$

where p is the spectral projection of $F(u)$ corresponding to the greatest eigenvalue.

Remark 4.1 *(Spectral representation of faces).* A proof is given in Section 3.2 of [25] that for $u \in \mathbb{R}^n$ the *support function* $h_{W(F)} := \max\{\langle x, u \rangle \mid x \in W(F)\}$ of $W(F)$ is the greatest eigenvalue of $F(u)$. This result goes back to Toeplitz [55] for $n = 2$. The same conclusion follows also from (2.3) and (4.2), in particular $h_{W(F)}(u) = \max\{\langle x, u\rangle \mid x \in L(F)\}$.

The generic convex support of at most three hermitian matrices is an oval.

Theorem 4.2. *Let $n \in \{1, 2, 3\}$ and $d \geq 2$. Then the set of n-tuples of hermitian d-by-d matrices $F \in (M_d^{\mathrm{h}})^n$ such that $L(F)$ is an oval is open and dense in $(M_d^{\mathrm{h}})^n$.*

Proof. For $n = 1, 2, 3$ and $d \in \mathbb{N}$ the set $\mathcal{O}_1$ of all $F \in (M_d^{\mathrm{h}})^n$ where every matrix in the pencil $\{F(u) \mid u \in \mathbb{R}^n \setminus \{0\}\}$ has d simple eigenvalues is open and dense in $(M_d^{\mathrm{h}})^n$, this was shown in Prop. 4.9 of [25]. Hence, for $F \in \mathcal{O}_1$ all proper exposed faces of $L(F)$ are singletons by (4.2). Secondly, since $n + 1 \leq \dim_{\mathbb{R}}(M_d^{\mathrm{h}}) = d^2$ holds by the assumptions $n \leq 3$ and $d \geq 2$, it is easy to prove that $\mathbb{1}_d, F_1, \ldots, F_n$ are linearly independent for F in an open and dense subset $\mathcal{O}_2$ of $(M_d^{\mathrm{h}})^n$, that is $\dim(L(F)) = n$ holds for $F \in \mathcal{O}_2$. The extreme rays of every normal cone of $L(F)$ are normal cones by Lemma 3.1. Hence Lemma 3.2 proves that $L(F)$ is an oval for all F in $\mathcal{O}_1 \cap \mathcal{O}_2$. The proof is completed by observing that in a metric space the intersection of two open and dense subsets is dense. □

Let us now focus on 3-by-3 matrices ($d = 3$). As explained earlier in this section, every proper exposed face of the state space $\mathcal{M}_3 = \mathcal{M}(M_3)$ is the state space $\mathcal{M}(pM_3p)$ of the algebra pM_3p for an orthogonal projection operator $p \in M_3$ of rank one or two. In the former case $\mathcal{M}(pM_3p)$ is a singleton and in the latter case a three-dimensional Euclidean ball. Hence (4.1) shows that every proper exposed face of the convex support $L(F)$ is a singleton, segment, filled ellipse, or filled ellipsoid.

Lemma 4.3. *Let F be an n-tuple of hermitian 3-by-3 matrices. Then every proper face of $L(F)$ is a singleton, segment, filled ellipse, or filled ellipsoid. If that face is no singleton then it is an exposed face of $L(F)$.*

Proof. Every proper face G of $L(F)$ lies in a proper exposed face H of $L(F)$ (see for example Lemma 4.6 of [57]), hence G is a face of H. As mentioned above, H is a singleton, segment, ellipse, or ellipsoid. If G is no singleton then $G = H$ since all proper faces of H are singletons. □

The next aim is to provide a method to certify that all large faces, defined in (1.1) for $d = n = 3$ were found. Therefore use the discriminant and a sum of squares decomposition of its absolute values.

Remark 4.4 *(Discriminant method).* Recall from (2.2) that $L(F) = \mathbb{E}_F(\mathcal{M}_3)$ is a projection of a state space. Hence, if the exposed face $\mathbb{F}_{L(F)}(u)$ of $L(F)$, defined by $u \in \mathbb{R}^3$, is a large face, then its pre-image $\mathbb{E}_F|_{\mathcal{M}_d}^{-1}(\mathbb{F}_{L(F)}(u))$ is necessarily no singleton. As we pointed out in equation (4.2) this means that the greatest eigenvalue of $F(u)$ is degenerate. The latter can be checked using a discriminant.

Let $a_1, a_2, a_3 \in \mathbb{C}$ and consider the polynomial $p(\lambda) = -\lambda^3 + a_1\lambda^2 + a_2\lambda + a_3$ of degree three. The *discriminant* of p, see Section A.1.2 of [22], is

$$-(27a_3^2 + 18a_1a_2a_3 - 4a_1^3a_3 + 4a_2^3 - a_1^2a_2^2).$$

Let $\lambda_1, \lambda_2, \lambda_3 \in \mathbb{C}$ denote the roots of p. Then the discriminant of p can be written

$$\Pi_{1\leq i<j\leq 3}(\lambda_i - \lambda_j)^2.$$

The *discriminant* $\delta(A)$ of a 3-by-3 matrix $A \in M_3$ is the discriminant of the characteristic polynomial $\det(A - \lambda\mathbb{1})$. So, A has a multiple eigenvalue if and only if $\delta(A) = 0$.

Let $Z \in M_3$ be a normal 3-by-3 matrix, that is $Z^*Z = ZZ^*$. The entries of the matrices $Z^0 = \mathbb{1}$, $Z^1 = Z$, and $Z^2 = ZZ$ can be combined to form a 9-by-3 matrix Z_*. Let an ordering of the nine indices $(i,j)_{i,j=1,\ldots,3}$ of a 3-by-3 matrix be given. In that order, the i-th column of Z_* is defined to contain the matrix coefficients of Z^i, $i = 0,1,2$. Now the absolute value of the discriminant of the normal matrix Z is the sum of squares [32]

$$|\delta(Z)| = \textstyle\sum_\nu |M_\nu|^2, \tag{4.3}$$

where the sum extends over the 84 three-element subsets $\nu \subset \{1,2,3\}\times\{1,2,3\}$ of indices of a 3-by-3 matrix and where M_ν is the minor of order 3-by-3 of Z_* formed by the rows indexed by ν. It is worth noting that the discriminant of a real symmetric 3-by-3 matrix can be decomposed into a sum of five squares [18].

Let $d, n \in \mathbb{N}$ be arbitrary. A proper exposed face G of $L(F) \subset \mathbb{R}^n$ which is no singleton has necessarily a pre-image $\mathbb{E}_F|_{\mathcal{M}_d}^{-1}(G)$ which is no singleton. We show now that this is sufficient for $d = 3$ with the exception of special Euclidean balls. To describe this problem more precisely we use for arbitrary $d, n \in \mathbb{N}$ an equivalence relation on $(M_d^{\mathrm{h}})^n$. For $F = (F_1, \ldots, F_n) \in (M_d^{\mathrm{h}})^n$ and a unitary $U \in M_d$ let $U^*FU := (U^*F_1U, \ldots, U^*F_nU)$. Two tuples $F, G \in (M_d^{\mathrm{h}})^n$ are equivalent if and only if either

$$G = U^*FU \text{ holds for some unitary } U \in M_d$$

or

$$\mathbb{1}_d, G_1, \ldots, G_n \text{ and } \mathbb{1}_d, F_1, \ldots, F_n \text{ have the same span.}$$

The first condition means that the equivalence classes are invariant under unitary similarity with any unitary $U \in M_d$,

$$(M_d^{\mathrm{h}})^n \to (M_d^{\mathrm{h}})^n, \quad F \mapsto U^* F U. \tag{4.4}$$

The convex support is invariant under these transformations, $L(U^*FU) = L(F)$. The second condition means that the classes are invariant under the action of the affine group of $\mathbb{R}^n$. More precisely, let $A = (a_{i,j}) \in \mathbb{R}^{n\times n}$ be an invertible matrix and $b \in \mathbb{R}^n$. There are two affine transformations

$$\alpha : \mathbb{R}^n \to \mathbb{R}^n, \quad x \mapsto (\textstyle\sum_{j=1}^n a_{i,j}x_j + b_i)_{i=1}^n \tag{4.5}$$

and

$$\beta : (M_d^{\mathrm{h}})^n \to (M_d^{\mathrm{h}})^n, \quad F \mapsto (\textstyle\sum_{j=1}^n a_{i,j}F_j + b_i \mathbb{1}_d)_{i=1}^n. \tag{4.6}$$

Notice that $\alpha \circ \mathbb{E}_F(X) = \mathbb{E}_{\beta(F)}(X)$ holds whenever $X \in M_d^{\mathrm{h}}$ has trace one. This implies $\alpha(L(F)) = L(\beta(F))$, which means that convex support sets and n-tuples of hermitian matrices transform equivariant under the affine group of $\mathbb{R}^n$.

Lemma 4.5. *Let $n \in \mathbb{N}$, $F \in (M_3^{\mathrm{h}})^n$, $D := \dim(L(F))$, $D \geq 1$, and assume that the pre-image of some exposed point of $L(F)$ under $\mathbb{E}_F|_{\mathcal{M}_3}$ is no singleton.*

Then $D \leq 5$ and F is equivalent modulo (4.4) and (4.6) to $G = (G_1, \ldots, G_n)$ where

$$G_1 = \begin{pmatrix} 1 & 0 & 0 \\ 0 & 1 & 0 \\ 0 & 0 & -1 \end{pmatrix}, \qquad G_i = \begin{pmatrix} 0 & 0 & a_i \\ 0 & 0 & b_i \\ \overline{a_i} & \overline{b_i} & 0 \end{pmatrix}, \quad 2 \leq i \leq D, \qquad \text{and} \quad G_i = 0, \quad D < i \leq n$$

holds for some vectors $v_i = \binom{a_i}{b_i} \in \mathbb{C}^2$, $i = 2, \ldots, D$. If $D \leq 4$ then there are $\varphi, \theta \in [0, \pi)$ such that modulo (4.4) and (4.6) one can choose

$$v_2 = \binom{1}{0}, \quad v_3 = \binom{\mathrm{i}\cos(\varphi)}{\sin(\varphi)}, \quad \text{and} \quad v_4 = \cos(\theta)\binom{-\mathrm{i}\sin(\varphi)}{\cos(\varphi)} + \sin(\theta)\binom{0}{\mathrm{i}}. \tag{4.7}$$

If $D = 5$ then one can take

$$v_2 = \binom{1}{0}, \quad v_3 = \binom{\mathrm{i}}{0}, \quad v_4 = \binom{0}{1}, \quad \text{and} \quad v_5 = \binom{0}{\mathrm{i}}. \tag{4.8}$$

If the matrices F are real symmetric then necessarily $D \leq 3$ and one can choose

$$v_2 = \binom{1}{0} \quad \text{and} \quad v_3 = \binom{0}{1}. \tag{4.9}$$

In any of the cases (4.7), (4.8), or (4.9) the convex support $L(G)$ is the cartesian product $B^D \times \{o\}$ of the unit ball $B^D = \{y \in \mathbb{R}^D \mid y_1^2 + \cdots + y_D^2 \leq 1\}$ of $\mathbb{R}^D$ with the origin $o = (0, \ldots, 0)$ of $\mathbb{R}^{n-D}$. The pre-image $\mathbb{E}_G|_{\mathcal{M}_3}^{-1}(1, 0, \ldots, 0)$ is a three-dimensional Euclidean ball and the pre-images of all other exposed points of $L(G)$ are singletons.

Proof. Let x be an exposed point of $L(F)$, say $\{x\} = \mathbb{F}_{L(F)}(u)$ for a unit vector $u \in \mathbb{R}^n$. Applying a rotation (4.6) of $\mathbb{R}^n$ we take $u := (1, 0, \ldots, 0)$. By (4.2) the pre-image of x is $\mathbb{E}_F|_{\mathcal{M}_3}^{-1}(x) = \mathcal{M}(p\mathcal{M}_3 p)$ where p is the spectral projection of $F(u) = F_1$ corresponding to the greatest eigenvalue. Since $\mathbb{E}_F|_{\mathcal{M}_3}^{-1}(x)$ is not a singleton and not equal to $\mathcal{M}_3$ it follows that p has rank two. For all $i = 1, \ldots, n$ the matrix $pF_i p$ is a scalar multiple of p. Otherwise one finds two states $\rho_1, \rho_2 \in \mathcal{M}(p\mathcal{M}_3 p)$ with $\langle \rho_1, F_i\rangle \neq \langle \rho_2, F_i\rangle$ for some i. But then $\{x\} = \mathbb{E}_F(\mathcal{M}(pM_3 p))$ cannot be a singleton. A unitary similarity (4.4) and another affine map (4.6) transform F into G defined in the statement of the lemma. For a unitary $U \in M_2$ consider the 3-by-3 unitary in block matrix form

$$V = \left(\begin{smallmatrix} U & 0 \\ 0 & 1 \end{smallmatrix}\right).$$

We have

$$VG_1V^* = G_1, \qquad \text{and} \quad V\begin{pmatrix} 0 & v_i \\ v_i^* & 0 \end{pmatrix}V^* = \begin{pmatrix} 0 & Uv \\ (Uv)^* & 0 \end{pmatrix}.$$

So the problem to further simplify the representation of G is to give a simple description of the $(D-1)$-frames of $\mathbb{C}^2$ with respect to the standard Euclidean scalar product of $\mathbb{C}^2$ as a real four-dimensional vector space modulo the action of $U(2)$ (but not of $O(4)$). This leads to the vectors v_i's in (4.7) and (4.8). If F is real symmetric, then all unitary similarities (4.4) can be realized with real orthogonal matrices. Then $D \leq 3$ follows and the v_i's may be chosen to be (4.9).

Let us analyze $L(G)$. Since $G_i = 0$ for $i > D$, it suffices to study $D = n$. Remark 4.1 shows that for $u \in \mathbb{R}^n$

$$h(u) := \max_{x \in L(G)} \langle u, x\rangle$$

is the greatest eigenvalue of $G(u) = u_1G_1 + \cdots + u_nG_n$. An easy computation shows that if u is a unit vector then the matrix $G(u)$ has eigenvalues $\{-1, u_1, 1\}$. So $h(u) = 1$ holds for all unit vectors $u \in \mathbb{R}^n$ and this shows that $L(G)$ is the unit ball B^n. Let $v := (1, 0, \ldots, 0) \in \mathbb{R}^n$. The pre-image $\mathbb{E}_G|_{\mathcal{M}_3}^{-1}(v)$ of the exposed face $\{v\} = \mathbb{F}_{L(G)}(v)$ of $L(G)$ is a three-dimensional ball since the greatest eigenvalue of G_1 is degenerate (4.2). To see that v is the unique exposed point of $L(G)$ with multiple pre-image points it suffices to show that $G(u)$ has no double eigenvalue for any unit vector $u \in \mathbb{R}^n$ which is not collinear with v. This can be seen from the discriminant $\delta(G(u)) = 4(u_2^2 + \cdots + u_n^2)^2$ of $G(u)$. □

It is worth to make an observation about n-tuples of 3-by-3 matrices $F \in (M_3^{\mathrm{h}})^n$ where $L(F)$ has an exposed point with multiple pre-images. It was shown in Theorem 3.2 of [39] for such tuples that if $\dim(L(F)) \leq 2$ then F is unitarily reducible. The same conclusion can be drawn from Lemma 4.5. With rare exceptions, the lemma shows also that if $\dim(L(F)) \geq 3$ then F is unitarily irreducible. The exceptions are those F where

$\dim(L(F)) = 3$ and where F is equivalent modulo (4.4) and (4.6) to an n-tuple G defined by $v_2 = \binom{1}{0}$ and $v_3 = \binom{\mathrm{i}}{0}$ of equation (4.7) or (4.8).

While $L(F)$ is generically an oval for $n \leq 3$ and $d \geq 2$ (by Theorem 4.2) we now study non-ovals.

Lemma 4.6. *Let $F \in (M_3^{\mathrm{h}})^n$. If $\dim(L(F)) \geq 6$ ($\dim(L(F)) \geq 4$ suffices if the F_i's are real symmetric), then $L(F)$ is no oval.*

Proof. Notice that $n \geq \dim(L(F))$ holds. If $n \geq 4$ (resp. $n \geq 3$ for real symmetric matrices) then Theorem D (resp. Theorem B) of [23] proves that there is a non-zero $u \in \mathbb{R}^n$ such that $F(u) = u_1F_1 + \cdots + u_nF_n$ has a multiple eigenvalue. So the greatest eigenvalue of $F(v)$ is degenerate, either for $v = u$ or for $v = -u$. As we see from (4.2), this means that the exposed face $\mathbb{F}_{L(F)}(v)$ has multiple pre-image points under $\mathbb{E}_F|_{\mathcal{M}_3}$. If $L(F)$ is an oval, then $\mathbb{F}_{L(F)}(v)$ is a singleton and then Lemma 4.5 shows $n \leq 5$ ($n \leq 3$ if the matrices F are real symmetric). □

We finish the section with an analysis of corner points of a convex compact subset $C \subset \mathbb{R}^m$. As defined earlier, a point $x \in C$ is a *corner point* [21] of C if the normal cone $N(x)$ of C at x has dimension m. A point $x \in C$ is a *conical point* [8] of C if $C \subset x + K$ holds for a closed convex cone $K \subset \mathbb{R}^m$ containing no line. We denote the *polar* of a closed convex cone $K \subset \mathbb{R}^m$ by

$$K^\circ = \{u \in \mathbb{R}^m \mid \forall x \in K : \langle x, u\rangle \leq 0\}.$$

We recall that K° is a closed convex cone and $K = (K^\circ)^\circ$, see for example [53].

Lemma 4.7. *Let $C \subset \mathbb{R}^m$ be a convex compact subset and $x \in C$. Then x is a conical point of C if and only if x is a corner point C.*

Proof. For any point $x \in C$, the smallest closed convex cone containing $C - x$ is the polar $N(x)^\circ$ of the normal cone $N(x)$ of C at x, see for example equation (2.2) of [53]. So for an arbitrary closed convex cone $K \subset \mathbb{R}^m$ we have $C - x \subset K \iff N(x)^\circ \subset K$, that is

$$C \subset x + K \iff K^\circ \subset N(x).$$

The observation that K contains no line if and only if K° has full dimension m then proves the claim. □

The existence of corner points of $L(F)$ has strong algebraic consequences for F.

Lemma 4.8. *Let $F \in (M_3^{\mathrm{h}})^n$, and let p be a corner point of $L(F)$. Then F is unitarily reducible and there exists a non-zero vector $x \in \mathbb{C}^d$ such that $F_ix = p_ix$ holds for $i = 1, \ldots, n$.*

Proof. The equivalence of the notions of *conical point* and *corner point* is proved in Lemma 4.7. The remaining claims are proved in Proposition 2.5 of [8]. □

We derive a classification of corner points of $L(F)$ for 3-by-3 matrices.

Lemma 4.9. *Let $F \in (M_3^{\mathrm{h}})^n$, $D := \dim(L(F))$, and let $p \in \mathbb{R}^n$ be a corner point of $L(F)$. Then $D \in \{0, 1, 2, 3, 4\}$ and, ignoring $D = 0, 1$, the convex support $L(F)$ is the convex hull of the union of $\{p\}$*

- *($D = 2$) with a segment whose affine hull does not contain p or with an ellipse which contains p in its affine hull but not in its convex hull,*
- *($D = 3$) with an ellipse whose affine hull does not contain p or with an ellipsoid which contains p in its affine hull but not in its convex hull,*
- *($D = 4$) with an ellipsoid whose affine hull does not contain p.*

Proof. Lemma 4.8 proves that there exists a unitary $U \in M_3$ such that U^*FU has the block-diagonal form $U^*FU = (\,(p_1) \oplus G_1, \dots, (p_n) \oplus G_n\,)$ with $G \in (M_2^{\mathrm{h}})^n$. The convex support $L(F)$ is the convex hull of the union of $L(G)$ and $\{p\}$. Since $L(G)$ is a singleton, a segment, a filled ellipse, or a filled ellipsoid, only the cases listed above are possible. □

5. Arguments for the classification

We provide the arguments used in Theorem 1.1 to prove the classification of convex support sets $L(F)$ of three hermitian 3-by-3 matrices $F = (F_1, F_2, F_3)$. Throughout this section we take $d = n = 3$. We will be mainly concerned with intersections of large faces and with a graph embedding into their union.

Let $F \in (M_3^{\mathrm{h}})^3$. We recall from (1.1) that a large face of $L(F)$ is a proper exposed face of $L(F)$ which is no singleton. Equivalently, a large face is an exposed face of $L(F)$ of the form of a segment or of the form of an ellipse, but different from $L(F)$ itself. The set of large faces of $L(F)$ is denoted by $\mathcal{L}(F)$.

Let

$$P : \mathbb{R}^3 \to \mathbb{R}^2, \quad (x_1, x_2, x_3) \mapsto (x_1, x_2) \tag{5.1}$$

denote the projection onto the x_1-x_2-plane.

Lemma 5.1. *Let $F \in (M_3^{\mathrm{h}})^3$, let $G_1, G_2 \in \mathcal{L}(F)$, and $G_1 \neq G_2$. Then G_1 and G_2 intersect in a unique point. Modulo affine transformation (4.6), the images $P(G_1)$ and $P(G_2)$ in the x_1-x_2 plane are different one-dimensional faces of $L(F_1, F_2)$.*

Proof. The pre-image of G_i is of the form $\mathbb{E}_F|_{\mathcal{M}_3}^{-1}(G_i) = \mathcal{M}(p_i M_3 p_i)$ for $i = 1, 2$ where $p_i \in M_3$ is an orthogonal projection operator of rank two (4.2). Since the image of p_1 intersects the image of p_2, the exposed faces G_1 and G_2 intersect as well. The intersection point is unique for otherwise the two large faces would be equal (since they are segments or ellipses).

To study 2D projections of $L(F)$, let v_i be a unit normal vector of $L(F)$ at G_i for $i = 1, 2$. Notice that the existence of a large face implies $\dim(L(F)) \geq 2$. In case $\dim(L(F)) = 2$ we further require that translations by v_1 and v_2 preserve the affine hull of $L(F)$. Then v_1 and v_2 span a two-dimensional subspace $U \subset \mathbb{R}^3$. We choose an orthogonal transformation (4.5) which rotates U into the x_1-x_2-plane. We label the image of the exposed face G_i under that rotation by G'_i, $i = 1, 2$. We label the image of the matrix F_i under the corresponding rotation (4.6) by F'_i, $i = 1, 2, 3$. Then $G'_1 \neq G'_2$ are intersecting large faces of $L(F'_1, F'_2, F'_3)$. Since $L(F'_1, F'_2) = P(L(F'_1, F'_2, F'_3))$, the convex sets $P(G'_1)$ and $P(G'_2)$ are intersecting proper exposed faces of $L(F'_1, F'_2)$. We finish the proof by showing that $P(G'_1) \neq P(G'_2)$ have dimension one. Indeed, if $P(G'_1) = P(G'_2)$ then the contradiction $G'_1 = G'_2$ follows. Otherwise, if $P(G'_1)$ is a singleton, then $P(G'_1) \subset P(G'_2)$ follows and now $G'_1 \subset G'_2$ contradicts the assumption that $G'_1 \neq G'_2$ are large faces. The case where $P(G'_2)$ is a singleton is analogous. □

Next we look at the convex support $L(F)$ of $F \in (M_3^{\mathrm{h}})^3$ which has no corner points. Triples $G_1, G_2, G_3 \in \mathcal{L}(F)$ of mutually distinct large faces satisfy the second assumptions of the next lemma and hence have no points in common.

Lemma 5.2. *Let $C \subset \mathbb{R}^3$ be a convex subset without corner point. Let G_1, G_2, G_3 be proper exposed faces of C, none of which is included in any of the others. Then $G_1 \cap G_2 \cap G_3 = \emptyset$.*

Proof. We prove the assertion by contradiction and assume that $G = G_1 \cap G_2 \cap G_3$ is non-empty. Since $L(F)$ has no corner points we have $\dim(N(G)) \leq 2$. As G is strictly included in G_i for $i = 1, 2, 3$, the antitone lattice isomorphism (3.2) shows that $N(G_i)$ is strictly included in $N(G)$. Proposition 4.8 of [57] shows that $N(G_i)$ is a proper face of $N(G)$, so $\dim(N(G_i)) < \dim(N(G)) \leq 2$ holds for $i = 1, 2, 3$. Since the G_i are proper exposed faces of $L(F)$ we have $\dim(N(G_i)) \geq 1$. Summarizing the dimension count, we have $\dim(N(G_i)) = 1$ for $i = 1, 2, 3$ and $\dim(N(G)) = 2$. But this is a contradiction, as a two-dimensional convex cone cannot have three one-dimensional faces. □

The two preceding lemmas allow a complete graph to be embedded into the union of large faces.

Lemma 5.3 *(Graph embedding). Let $F \in (M_3^{\mathrm{h}})^3$, let $L(F)$ have no corner point, and let k be the number of large faces of $L(F)$. Then the complete graph on k vertices embeds into the union of large faces such that there is one vertex on each large face.*

Proof. For each $G \in \mathcal{L}(F)$ we denote by $c(G)$ the centroid of G and we take it as a vertex of the graph. Lemma 5.1 shows that each two distinct $G, H \in \mathcal{L}(F)$ intersect in a unique point $p(G, H)$. We define the edge between $c(G)$ and $c(H)$ as the union of two segments, one segment between $c(G)$ and $p(G, H)$ and another between $p(G, H)$ and $c(H)$. We finish the proof by showing that distinct edges intersect at most in one of their vertices. Consider the first pair of vertices $c(G_1)$ and $c(H_1)$ and the second pair $c(G_2)$ and $c(H_2)$, defined by $G_1, G_2, H_1, H_2 \in \mathcal{L}(F)$. If the edge between $c(G_1)$ and $c(H_1)$ intersects the edge between $c(G_2)$ and $c(H_2)$ outside of one of the vertices $c(G_1), c(G_2), c(H_1), c(H_2)$, then $p(G_1, H_1) = p(G_2, H_2)$ follows because intersection points between large faces are unique by Lemma 5.1. However, if $p(G_1, H_1) = p(G_2, H_2)$ then Lemma 5.2 shows $\{G_1, H_1\} = \{G_2, H_2\}$ which means that the two edges are equal. □

Two segments in $\mathcal{L}(F)$ produce a corner point of $L(F)$ at their intersection.

Lemma 5.4. *Let $F \in (M_3^{\mathrm{h}})^3$ and let there be two distinct segments in $\mathcal{L}(F)$. Then $L(F)$ has a corner point.*

Proof. Lemma 5.1 proves that, after an affine transformation, the two segments in $\mathcal{L}(F)$ project under the projection P onto the x_1-x_2-plane (5.1) to two one-dimensional faces of $L(F_1, F_2)$. The classification of the numerical range of a 3-by-3 matrix [35] shows that either $L(F_1, F_2)$ is a triangle or the convex hull of an ellipse and a point outside the ellipse.

In the first case where $L(F_1, F_2)$ is a triangle, another affine transformation allows us to assume

$$F_1 = \mathrm{diag}(0, -1, 0) \quad \text{and} \quad F_2 = \mathrm{diag}(0, 0, -1)$$

where $L(F_1, F_2)$ is the triangle with vertices $(0, 0)$, $(-1, 0)$, and $(0, -1)$. Assuming further that the exposed faces $\mathbb{F}_{L(F)}(1, 0, 0)$ and $\mathbb{F}_{L(F)}(0, 1, 0)$ of $L(F)$ are segments, we prove that the pre-image $P|_{L(F)}^{-1}(0, 0)$ of the origin of $\mathbb{R}^2$ is a corner point of $L(F)$. Equation (4.2) shows that the segment $\mathbb{F}_{L(F)}(1, 0, 0)$, respectively $\mathbb{F}_{L(F)}(0, 1, 0)$, is the image of a three-dimensional ball $\mathcal{M}(p_1 M_3 p_1)$, respectively $\mathcal{M}(p_2 M_3 p_2)$, with $p_1 := \mathrm{diag}(1, 0, 1)$, respectively $p_2 := (1, 1, 0)$. Let $v := (1, 0, 0)$, $v_1 := (0, 0, 1)$, and $v_2 := (0, 1, 0)$. The matrix of $p_1 F_2 p_1$ in the basis (v, v_1) is $\mathrm{diag}(0, -1)$. Since $\mathbb{F}_{L(F)}(1, 0, 0)$ is a segment, $p_1 F_3 p_1$ must be a linear combination of p_1, $0 = p_1 F_1 p_1$, and $p_1 F_2 p_1$. Therefore the off-diagonal terms $\langle v, F_3 v_1 \rangle = (F_3)_{1,3}$ and $\langle v_1, F_3 v \rangle = \overline{(F_3)_{1,3}}$ vanish. Analogously, since $\mathbb{F}_{L(F)}(0, 1, 0)$ is a segment we have $(F_3)_{1,2} = (F_3)_{2,1} = 0$. This proves that F is unitarily reducible of the form

$$F_1 = \left(\begin{array}{c|cc} 0 & 0 & 0 \\ \hline 0 & \multicolumn{2}{c}{\multirow{2}{*}{G_1}} \\ 0 & & \end{array}\right), \quad F_2 = \left(\begin{array}{c|cc} 0 & 0 & 0 \\ \hline 0 & \multicolumn{2}{c}{\multirow{2}{*}{G_2}} \\ 0 & & \end{array}\right), \quad F_3 = \left(\begin{array}{c|cc} a & 0 & 0 \\ \hline 0 & \multicolumn{2}{c}{\multirow{2}{*}{G_3}} \\ 0 & & \end{array}\right)$$

where $a = (F_3)_{1,1}$ and $G = (G_1, G_2, G_3) \in (M_2^{\mathrm{h}})^3$. It is easy to see that $(0, 0, a)$ is a corner point of $L(F)$ because $L(F)$ is the convex hull of the union of the point $(0, 0, a)$ and of $L(G)$ which projects to the segment

$$P(L(G)) = [(-1,0),(0,-1)] = L(G_1,G_2)$$

in the x_1-x_2 plane.

Similarly we argue in the second case when $L(F_1, F_2)$ is the convex hull of an ellipse and a point outside the ellipse. Here, we have several affinely inequivalent cases. Lemma 5.1 of [54] proves that there is $a > 1$ such that (F_1, F_2) is equivalent modulo affine transformation (4.6) to (F_1', F_2'), where

$$F_1' = \begin{pmatrix} 0 & 1 & 0 \\ 1 & 0 & 0 \\ 0 & 0 & a \end{pmatrix} \quad \text{and} \quad F_2' = \begin{pmatrix} 0 & -\mathrm{i} & 0 \\ \mathrm{i} & 0 & 0 \\ 0 & 0 & 0 \end{pmatrix}.$$

Another affine transformation allows us to assume that the matrices F_1 and F_2 are of the form

$$F_1 = F_1' + \sqrt{a^2-1}F_2' \quad \text{and} \quad F_2 = F_1' - \sqrt{a^2-1}F_2'.$$

The new matrices F_1 and F_2 have the same eigenvalues $(-a, a, a)$. The eigenvectors of F_1, respectively F_2, corresponding to a are $v := (0, 0, 1)$ and

$$v_1 := ((1-\mathrm{i}\sqrt{a^2-1})/a, 1, 0), \quad \text{respectively} \quad v_2 := ((1+\mathrm{i}\sqrt{a^2-1})/a, 1, 0).$$

As in the first case, the off-diagonal entries $\langle v_1, F_3 v\rangle$ and $\langle v_2, F_3 v\rangle$ vanish. So F is unitarily reducible and $(a, a, (F_3)_{3,3})$ is a corner point of $L(F)$. □

6. Examples

We analyze and depict examples of convex support sets $L(F)$ of three hermitian 3-by-3 matrices which have dimension three and no corner points. Thereby we prove that the corresponding eight classes of Fig. 2 are populated.

For all examples we write down the outer normal vectors $u \in \mathbb{R}^3$ of all candidates of large faces and we provide witnesses (hermitian squares) that there are no other large faces. This is explained in Example 6.2. Later on the normal vector and witnesses are simply listed. We omit to verify that the candidates are indeed large faces. The proof is a straightforward computation with 2-by-2 matrices (4.2): If $F(u)$ has a maximal eigenvalue with spectral projection p then the exposed face $\mathbb{F}_{L(F)}(u)$ is the convex support of the compressions of F_1, F_2, F_3 to the range of p.

The graphics of Figs. 3 and 4 were computed with Wolfram Mathematica using a heuristic method for which we have no proof of correctness.

Remark 6.1 *(Drawing method for convex support sets).* Recall from Remark 1.2 the definition of the complex projective hypersurface S_F in $\mathbb{P}^3$ with defining polynomial $p(u_0, u_1, u_2, u_3) := \det(u_0\mathbb{1} + u_1F_1 + u_2F_2 + u_3F_3)$, its dual variety S_F^* in $\mathbb{P}^3$, and the

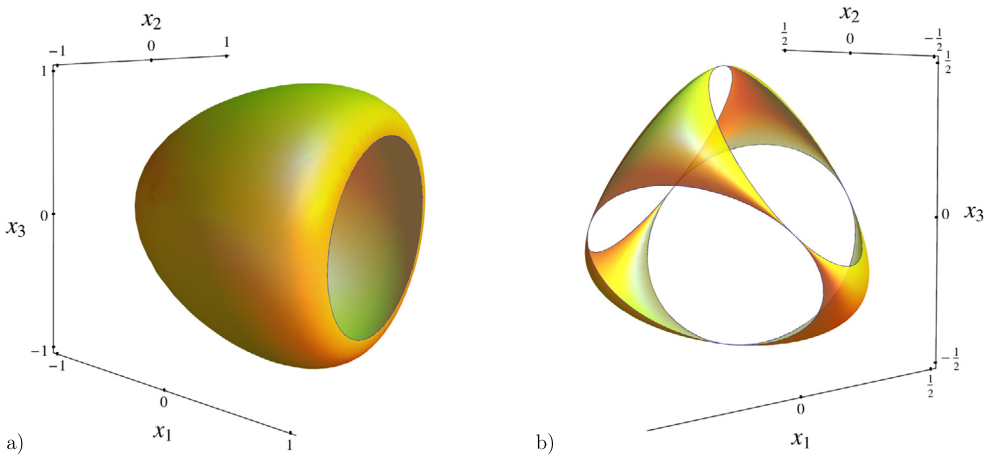

Fig. 3. a) Object with one ellipse and b) object with four ellipses at the boundary. The depicted surfaces are the pieces of the boundary generating surfaces which lie on the boundary of the convex support.

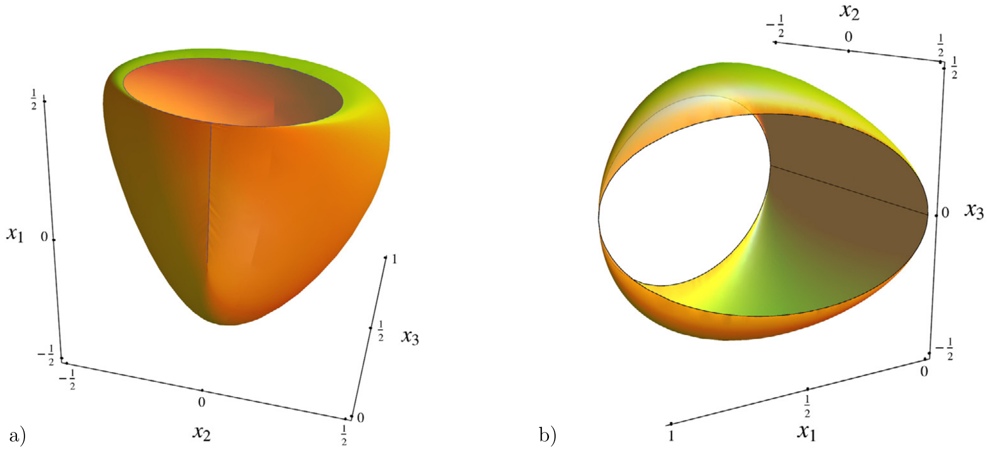

Fig. 4. a) Object with one segment and one ellipse and b) object with one segment and two ellipses. The depicted surfaces are the pieces of the boundary generating surfaces which lie on the boundary of the convex support.

boundary generating surface $S_F^\wedge(\mathbb{R})$ in $\mathbb{R}^3$. For the following examples the dual S_F^* is also a hypersurface and we find its defining polynomial $\tilde{q}(x_0, x_1, x_2, x_3)$ by computing the Gauss image [27] of the hypersurface S_F, which we do by computing a Groebner basis of the ideal generated by

$$p, \qquad \partial_{u_i} p - x_i, \quad i = 0, 1, 2, 3,$$

with the variables (u_0, u_1, u_2, u_3) eliminated. The boundary generating surface $S_F^\wedge(\mathbb{R})$ is the zero set in $\mathbb{R}^3$ of the polynomial

$$q(x_1, x_2, x_3) := \tilde{q}(1, x_1, x_2, x_3). \tag{6.1}$$

It is false that the convex hull of $S_F^\wedge(\mathbb{R})$ is the convex support $L(F)$, because the surface $S_F^\wedge(\mathbb{R})$ can contain straight lines [15].

Notice that the polynomials $\partial_{u_i} p - x_i$ are inhomogeneous and do not define a projective variety in $\mathbb{P}^7$. Alternatively, Algorithm 5.1 of [51] uses the homogeneous 2-by-2 minors of the matrix

$$\begin{pmatrix} x_0 & x_1 & x_2 & x_3 \\ \partial_{u_0} p & \partial_{u_1} p & \partial_{u_2} p & \partial_{u_3} p \end{pmatrix}$$

and a suitable saturation ideal.

We now discuss a three-dimensional example for each class of Fig. 2 except for the class $(0,0)$ of ovals where we refer to Section 4 of [36].

Example 6.2 *(No segment, one ellipse).* See Fig. 1a) for a printout and Fig. 3a) for a drawing.

$$F_1 := \begin{pmatrix} 1 & 0 & 0 \\ 0 & 1 & 0 \\ 0 & 0 & -1 \end{pmatrix}, \quad F_2 := \tfrac{1}{\sqrt{2}} \begin{pmatrix} 0 & 1 & 0 \\ 1 & 0 & 1 \\ 0 & 1 & 0 \end{pmatrix}, \quad F_3 := \tfrac{1}{\sqrt{2}} \begin{pmatrix} 0 & -\mathrm{i} & 0 \\ \mathrm{i} & 0 & -\mathrm{i} \\ 0 & \mathrm{i} & 0 \end{pmatrix},$$

$$q = -4x_1^3 - 4x_1^4 + 27x_2^2 + 18x_1x_2^2 - 13x_1^2x_2^2 - 32x_2^4 + 27x_3^2 + 18x_1x_3^2 - 13x_1^2x_3^2 - 64x_2^2x_3^2 - 32x_3^4.$$

The sum of squares representation (4.3) of the modulus of the discriminant of $F(u)$ contains the term

$$|M_\nu|^2 = (u_2^2 + u_3^2)^3/8$$

corresponding to $\nu := \{(1,1), (1,2), (1,3)\}$. This term vanishes only for $u_2 = u_3 = 0$. Thus Remark 4.4 shows that $\mathbb{F}_{L(F)}(1,0,0)$ and $\mathbb{F}_{L(F)}(-1,0,0)$ are the only candidates for large faces of $L(F)$. A direct computation proves that $\mathbb{F}_{L(F)}(1,0,0)$ is an ellipse (hence $\mathbb{F}_{L(F)}(-1,0,0)$ is a singleton).

Example 6.3 *(No segment, two ellipses).*

$$F_1 := \begin{pmatrix} 1 & 0 & 0 \\ 0 & -1 & 0 \\ 0 & 0 & 0 \end{pmatrix}, \quad F_2 := \begin{pmatrix} 0 & 0 & 1 \\ 0 & 0 & 0 \\ 1 & 0 & 0 \end{pmatrix}, \quad F_3 := \begin{pmatrix} 0 & 1 & 0 \\ 1 & 0 & 0 \\ 0 & 0 & 0 \end{pmatrix},$$

$$q = 4x_1x_2^2 - 4x_1^2x_2^2 - x_2^4 + 4x_3^2 - 4x_1^2x_3^2 - 4x_2^2x_3^2 - 4x_3^4.$$

The hermitian squares corresponding to $\nu_1 := \{(1,1), (1,2), (3,3)\}$, $\nu_2 := \{(1,1), (1,3), (2,2)\}$, and $\nu_3 := \{(1,1), (2,2), (3,3)\}$ are

$$
\begin{aligned}
&|M_{\nu_1}|^2 = (1+u_1^2)^2, && \text{if } u_3 = 1,\\
&|M_{\nu_2}|^2 = u_2^2(u_2^2 - 2u_1^2)^2, && \\
\text{and}\quad &|M_{\nu_3}|^2 = u_1^2(u_2^2 - 2u_1^2)^2, && \text{if } u_3 = 0.
\end{aligned}
$$

Thus, $\mathbb{F}_{L(F)}(-1, \pm\sqrt{2}, 0)$ are the unique large faces of $L(F)$.

Example 6.4 *(No segment, three ellipses).* See Fig. 1b) for a printout of $L(F)$ corresponding to the matrices (6.2). The first instance of an object without segment and with three ellipses which we found was

$$
F_1 := \begin{pmatrix} 0&1&0\\ 1&0&0\\ 0&0&0 \end{pmatrix}, \quad F_2 := \tfrac{1}{\sqrt{2}}\begin{pmatrix} 0&\mathrm{i}&1\\ -\mathrm{i}&0&0\\ 1&0&0 \end{pmatrix}, \quad F_3 := \begin{pmatrix} 1&0&0\\ 0&1&0\\ 0&0&-1 \end{pmatrix},
$$
$$
\begin{aligned}
q = &-4x_1^6 - 24x_1^4x_2^2 + 27x_2^4 - 48x_1^2x_2^4 - 32x_2^6 + 36x_1^2x_2^2x_3 + 18x_2^4x_3 + 8x_1^4x_3^2\\
&- 4x_1^2x_2^2x_3^2 - 13x_2^4x_3^2 - 4x_2^2x_3^3 - 4x_1^2x_3^4 - 4x_2^2x_3^4.
\end{aligned}
$$

The hermitian squares corresponding to $\nu_1 := \{(1,1), (1,2), (2,2)\}$ and $\nu_2 := \{(1,1), (1,2), (3,3)\}$ are

$$
\begin{aligned}
&|M_{\nu_1}|^2 = (1+2u_1^2)/8, && \text{if } u_2 = 1,\\
\text{and}\quad &|M_{\nu_2}|^2 = u_1^2(u_1^2 - 4u_3^2)^2, && \text{if } u_2 = 0.
\end{aligned}
$$

Thus, $\mathbb{F}_{L(F)}(0,0,1)$, and $\mathbb{F}_{L(F)}(\pm 2, 0, -1)$ are the unique large faces of $L(F)$. Out of curiosity we mention also the example

$$
F_1 := \begin{pmatrix} 1&0&0\\ 0&0&1\\ 0&1&0 \end{pmatrix}, \quad F_2 := \begin{pmatrix} 0&1&0\\ 1&0&0\\ 0&0&1 \end{pmatrix}, \quad F_3 := \begin{pmatrix} 0&0&\mathrm{i}\\ 0&1&0\\ -\mathrm{i}&0&0 \end{pmatrix}. \tag{6.2}
$$

Here the normal vectors of the three ellipses are mutually orthogonal and $q(x_1, x_2, x_3)$ is a degree six polynomial with the maximal number of 84 monomials.

Example 6.5 *(No segment, four ellipses).* This example has appeared in [31]. See Fig. 1c) for a printout and Fig. 3b) for a drawing.

$$
F_1 := \tfrac{1}{2}\begin{pmatrix} 0&1&0\\ 1&0&0\\ 0&0&0 \end{pmatrix}, \quad F_2 := \tfrac{1}{2}\begin{pmatrix} 0&0&1\\ 0&0&0\\ 1&0&0 \end{pmatrix}, \quad F_3 := \tfrac{1}{2}\begin{pmatrix} 0&0&0\\ 0&0&1\\ 0&1&0 \end{pmatrix},
$$
$$
q = x_1x_2x_3 - x_1^2x_2^2 - x_1^2x_3^2 - x_2^2x_3^2.
$$

The surface $\{x \in \mathbb{R}^3 \mid q(x) = 0\}$ is also known as the Roman surface. For all unit vectors $u \in \mathbb{R}^3$ the discriminant of $F(u)$ is

$$
\begin{aligned}
\delta(F(u)) = &\tfrac{1}{32}((u_1^2 - u_2^2)^2 + (u_2^2 - u_3^2)^2 + (u_3^2 - u_1^2)^2\\
&+ 6(u_3^2(u_1^2 - u_2^2)^2 + u_1^2(u_2^2 - u_3^2)^2 + u_2^2(u_3^2 - u_1^2)^2)).
\end{aligned}
$$

Thus (4.2) proves that

$$\begin{aligned} &\mathbb{F}_{L(F)}(-1,-1,-1), && \mathbb{F}_{L(F)}(-1,1,1), \\ &\mathbb{F}_{L(F)}(1,-1,1), \quad \text{and} && \mathbb{F}_{L(F)}(1,1,-1) \end{aligned}$$

are the unique large faces of $L(F)$.

Example 6.6 *(One segment, no ellipses).* See Fig. 1d) for a printout.

$$F_1 := \begin{pmatrix} 0 & 1 & 0 \\ 1 & 0 & 0 \\ 0 & 0 & 0 \end{pmatrix}, \quad F_2 := \begin{pmatrix} 1 & 0 & 0 \\ 0 & -1 & 0 \\ 0 & 0 & 1 \end{pmatrix}, \quad F_3 := \tfrac{1}{\sqrt{2}} \begin{pmatrix} 0 & 0 & \mathrm{i} \\ 0 & 0 & 1 \\ -\mathrm{i} & 1 & 0 \end{pmatrix},$$

the polynomial q has degree eight and 31 monomials. The hermitian squares corresponding to $\nu_1 := \{(1,1), (1,2), (1,3)\}$ and $\nu_2 := \{(1,1), (1,2), (3,3)\}$ are

$$\begin{aligned} & |M_{\nu_1}|^2 = (1 + 4u_1^4 + 4u_1^2(1 + 4u_2^2))/8, && \text{if } u_3 = 1, \\ \text{and} \quad & |M_{\nu_2}|^2 = u_1^6, && \text{if } u_3 = 0. \end{aligned}$$

Thus, $\mathbb{F}_{L(F)}(0, 1, 0)$ is the unique large face of $L(F)$.

Example 6.7 *(One segment, one ellipse).* This object has appeared in [15]. Let

$$F_1 := \tfrac{1}{2} \begin{pmatrix} \lambda & 0 & 0 \\ 0 & 0 & 1 \\ 0 & 1 & 0 \end{pmatrix}, \quad F_2 := \tfrac{1}{2} \begin{pmatrix} 0 & 0 & 1 \\ 0 & 0 & 0 \\ 1 & 0 & 0 \end{pmatrix}, \quad F_3 := \begin{pmatrix} 0 & 0 & 0 \\ 0 & 0 & 0 \\ 0 & 0 & 1 \end{pmatrix},$$

$$q = -4x_1^2x_3^2 - 4x_2^2x_3^2 + 4x_3^3 - 4x_3^4 + 4x_1x_2^2x_3\lambda - x_2^4\lambda^2.$$

Unitary conjugation u^*F_1u, u^*F_2u, u^*F_3u with the diagonal matrix $\mathrm{diag}(\mathrm{i}, 1, 1)$ gives matrices whose convex support is, for $\lambda = 2$, affinely isomorphic to the example in Section 3 of [15]. See Fig. 1e) for a printout. A drawing at $\lambda = 1$ is depicted in Fig. 4a). Lemma 4.5 shows for $\lambda = 0$ that $L(F)$ is the ball of radius $\frac{1}{2}$ centered at $(0, 0, \frac{1}{2})$ and the origin is the unique boundary point whose pre-image is not a singleton. For $\lambda = 1$ the hermitian squares corresponding to $\nu_1 := \{(1,1), (1,2), (1,3)\}$, $\nu_2 := \{(1,1), (1,3), (2,2)\}$, and $\nu_3 := \{(1,1), (2,2), (2,3)\}$ are

$$\begin{aligned} & |M_{\nu_1}|^2 = u_1^2/64, && \text{if } u_2 = 1, \\ & |M_{\nu_2}|^2 = 1/64, && \text{if } u_2 = 1,\ u_1 = 0, \\ \text{and} \quad & |M_{\nu_3}|^2 = u_1^4u_3^2/16, && \text{if } u_2 = 0. \end{aligned}$$

Thus, $\mathbb{F}_{L(F)}(1, 0, 0)$ and $\mathbb{F}_{L(F)}(0, 0, -1)$ are the unique large faces of $L(F)$.

Example 6.8 *(One segment, two ellipses).* This object has appeared in [9]. Let

$$F_1 := \begin{pmatrix} 0&0&0 \\ 0&0&0 \\ 0&0&1 \end{pmatrix}, \quad F_2 := \tfrac{1}{2}\begin{pmatrix} 0&1&0 \\ 1&0&0 \\ 0&0&0 \end{pmatrix}, \quad F_3 := \tfrac{1}{2}\begin{pmatrix} 0&0&1 \\ 0&0&0 \\ 1&0&0 \end{pmatrix},$$
$$q = -x_1^2x_2^2 + x_1x_3^2 - x_1^2x_3^2 - x_3^4.$$

Orthogonal conjugation with the matrix $\begin{pmatrix} 1&1&0 \\ -1&1&0 \\ 0&0&\sqrt{2} \end{pmatrix}/\sqrt{2}$ produces matrices whose convex support is affinely isomorphic to Example 6 of [9]. See Fig. 1f) for a printout and Fig. 4b) for a drawing. The hermitian squares corresponding to $\nu_1 := \{(1,1), (1,3), (2,2)\}$ and $\nu_2 := \{(1,1), (1,2), (3,3)\}$ are

$$\begin{aligned} & |M_{\nu_1}|^2 = 1/64, && \text{if } u_3 = 1, \\ \text{and} \quad & |M_{\nu_2}|^2 = u_2^2(u_2^2 - 4u_1^2)^2/64, && \text{if } u_3 = 0. \end{aligned}$$

Thus, $\mathbb{F}_{L(F)}(-1, 0, 0)$ and $\mathbb{F}_{L(F)}(1, \pm 2, 0)$ are the unique large faces of $L(F)$. It is easy to find examples with one segment and two ellipses whose outer normal vectors are not coplanar.

References

[1] E.M. Alfsen, F.W. Shultz, State Spaces of Operator Algebras: Basic Theory, Orientations, and C*-Products, Birkhäuser, Boston, 2001.

[2] Y.H. Au-Yeung, Y.T. Poon, A remark on the convexity and positive definiteness concerning Hermitian matrices, Southeast Asian Bull. Math. 3 (1979) 85–92.

[3] G.P. Barker, The lattice of faces of a finite dimensional cone, Linear Algebra Appl. 7 (1973) 71–82.

[4] O. Barndorff-Nielsen, Information and Exponential Families in Statistical Theory, Wiley, Chichester, 1978.

[5] N. Bebiano, Nondifferentiable points of $\partial W_c(A)$, Linear Multilinear Algebra 19 (1986) 249–257.

[6] I. Bengtsson, S. Weis, K. Życzkowski, Geometry of the set of mixed quantum states: an apophatic approach, in: Geometric Methods in Physics, in: Trends in Mathematics, Birkhäuser, Basel, 2013, pp. 175–197.

[7] I. Bengtsson, K. Życzkowski, Geometry of Quantum States, II edition, Cambridge University Press, Cambridge, 2017.

[8] P. Binding, C.-K. Li, Joint ranges of Hermitian matrices and simultaneous diagonalization, Linear Algebra Appl. 151 (1991) 157–167.

[9] J. Chen, Z. Ji, C.-K. Li, Y.-T. Poon, Y. Shen, N. Yu, B. Zeng, D. Zhou, Discontinuity of maximum entropy inference and quantum phase transitions, New J. Phys. 17 (2015) 083019.

[10] J.-Y. Chen, Z. Ji, Z.-X. Liu, Y. Shen, B. Zeng, Geometry of reduced density matrices for symmetry-protected topological phases, Phys. Rev. A 93 (2016) 012309.

[11] J. Chen, C. Guo, Z. Ji, Y.-T. Poon, N. Yu, B. Zeng, J. Zhou, Joint product numerical range and geometry of reduced density matrices, Sci. China, Phys. Mech. Astron. 60 (2017) 020312.

[12] W.-S. Cheung, X. Liu, T.-Y. Tam, Multiplicities, boundary points, and joint numerical ranges, Oper. Matrices 1 (2011) 41–52.

[13] M.-T. Chien, H. Nakazato, Boundary generating curves of the c-numerical range, Linear Algebra Appl. 294 (1999) 67–84.

[14] M.-T. Chien, H. Nakazato, Flat portions on the boundary of the Davis–Wielandt shell of 3-by-3 matrices, Linear Algebra Appl. 430 (2009) 204–214.

[15] M.-T. Chien, H. Nakazato, Joint numerical range and its generating hypersurface, Linear Algebra Appl. 432 (2010) 173–179.

[16] M.-T. Chien, H. Nakazato, Singular points of the ternary polynomials associated with 4-by-4 matrices, Electron. J. Linear Algebra 23 (2012) 755–769.
[17] B. Collins, P. Gawron, A.E. Litvak, K. Życzkowski, Numerical range for random matrices, J. Math. Anal. Appl. 418 (2014) 516–533.
[18] M. Domokos, Discriminant of symmetric matrices as a sum of squares and the orthogonal group, Comm. Pure Appl. Math. 64 (2011) 443–465.
[19] C.F. Dunkl, P. Gawron, J.A. Holbrook, J. Miszczak, Z. Puchała, K. Życzkowski, Numerical shadow and geometry of quantum states, J. Phys. A: Math. Theor. 44 (2011) 335301.
[20] A. Dvoretzky, Some results on convex bodies and Banach spaces, in: Proc. Internat. Sympos. Linear Spaces, Jerusalem, 1961, pp. 123–160.
[21] M. Fiedler, Geometry of the numerical range of matrices, Linear Algebra Appl. 37 (1981) 81–96.
[22] G. Fischer, Plane Algebraic Curves, AMS, Providence, Rhode Island, 2001.
[23] S. Friedland, J.W. Robbin, J.H. Sylvester, On the crossing rule, Comm. Pure Appl. Math. 37 (1984) 19–37.
[24] I.M. Gelfand, M.M. Kapranov, A.V. Zelevinsky, Discriminants, Resultants, and Multidimensional Determinants, Birkhäuser Boston, Boston, 1994.
[25] E. Gutkin, E.A. Jonckheere, M. Karow, Convexity of the joint numerical range: topological and differential geometric viewpoints, Linear Algebra Appl. 376 (2004) 143–171.
[26] E. Gutkin, K. Życzkowski, Joint numerical ranges, quantum maps, and joint numerical shadows, Linear Algebra Appl. 438 (2013) 2394–2404.
[27] J. Harris, Algebraic Geometry: A First Course, Corr. 3rd print, Springer, New York, 1995.
[28] F. Hausdorff, Der Wertvorrat einer Bilinearform, Math. Z. 3 (1919) 314–316.
[29] J.W. Helton, I.M. Spitkovsky, The possible shapes of numerical ranges, Oper. Matrices 6 (2012) 607–611.
[30] D. Henrion, Semidefinite geometry of the numerical range, Electron. J. Linear Algebra 20 (2010) 322–332.
[31] D. Henrion, Semidefinite representation of convex hulls of rational varieties, Acta Appl. Math. 115 (2011) 319–327.
[32] N.V. Ilyushechkin, Discriminant of the characteristic polynomial of a normal matrix, Math. Notes 51 (1992) 230–235.
[33] L. Jakóbczyk, M. Siennicki, Geometry of Bloch vectors in two-qubit system, Phys. Lett. A 286 (2001) 383–390.
[34] D.S. Keeler, L. Rodman, I.M. Spitkovsky, The numerical range of 3×3 matrices, Linear Algebra Appl. 252 (1997) 115–139.
[35] R. Kippenhahn, Über den Wertevorrat einer Matrix, Math. Nachr. 6 (1951) 193–228.
[36] N. Krupnik, I.M. Spitkovsky, Sets of matrices with given joint numerical range, Linear Algebra Appl. 419 (2006) 569–585.
[37] P. Kurzyński, A. Kołodziejski, W. Laskowski, M. Markiewicz, Three-dimensional visualization of a qutrit, Phys. Rev. A 93 (2016) 062126.
[38] S.K. Goyal, B.N. Simon, R. Singh, S. Simon, Geometry of the generalized Bloch sphere for qutrits, J. Phys. A: Math. Theor. 49 (2016) 165203.
[39] T. Leake, B. Lins, I.M. Spitkovsky, Pre-images of boundary points of the numerical range, Oper. Matrices 8 (2014) 699–724.
[40] C.-K. Li, A simple proof of the elliptical range theorem, Proc. Amer. Math. Soc. 124 (1996) 1985–1986.
[41] C.-K. Li, Y.-T. Poon, Convexity of the joint numerical range, SIAM J. Matrix Anal. Appl. 21 (2000) 668–678.
[42] R. Loewy, B.-S. Tam, Complementation in the face lattice of a proper cone, Linear Algebra Appl. 79 (1986) 195–207.
[43] V. Müller, The joint essential numerical range, compact perturbations, and the Olsen problem, Studia Math. 197 (2010) 275–290.
[44] J. von Neumann, E.P. Wigner, Über das Verhalten von Eigenwerten bei adiabatischen Prozessen, Phys. Z. 30 (1929) 467–470.
[45] B. Polyak, Convexity of quadratic transformations and its use in control and optimization, J. Optim. Theory Appl. 99 (1998) 553–583.
[46] Z. Puchała, J.A. Miszczak, P. Gawron, C.F. Dunkl, J.A. Holbrook, K. Życzkowski, Restricted numerical shadow and geometry of quantum entanglement, Linear Algebra Appl. 479 (2015) 12–51.
[47] P.X. Rault, T. Sendova, I.M. Spitkovsky, 3-by-3 matrices with elliptical numerical range revisited, Electron. J. Linear Algebra 26 (2013) 158–167.

[48] G. Ringel, J.W.T. Youngs, Solution of the Heawood map-coloring problem, Proc. Natl. Acad. Sci. USA 60 (1968) 438–445.
[49] L. Rodman, I.M. Spitkovsky, 3×3 matrices with a flat portion on the boundary of the numerical range, Linear Algebra Appl. 397 (2005) 193–207.
[50] L. Rodman, I.M. Spitkovsky, A. Szkoła, S. Weis, Continuity of the maximum-entropy inference: convex geometry and numerical ranges approach, J. Math. Phys. 57 (2016) 015204.
[51] P. Rostalski, B. Sturmfels, Dualities, in: G. Blekherman, P. Parrilo, R. Thomas (Eds.), Semidefinite Optimization and Convex Algebraic Geometry, SIAM, Philadelphia, 2012, pp. 203–250.
[52] G. Sarbicki, I. Bengtsson, Dissecting the qutrit, J. Phys. A: Math. Theor. 46 (2013) 035306.
[53] R. Schneider, Convex Bodies: The Brunn–Minkowski Theory, Cambridge University Press, New York, 2014.
[54] I.M. Spitkovsky, S. Weis, Pre-images of extreme points of the numerical range, and applications, Oper. Matrices 10 (2016) 1043–1058.
[55] O. Toeplitz, Das algebraische Analogon zu einem Satze von Fejér, Math. Z. 2 (1918) 187–197.
[56] S. Weis, Quantum convex support, Linear Algebra Appl. 435 (2011) 3168–3188.
[57] S. Weis, A note on touching cones and faces, J. Convex Anal. 19 (2012) 323–353.
[58] V. Zauner, D. Draxler, Y. Lee, L. Vanderstraeten, J. Haegeman, F. Verstraete, Symmetry breaking and the geometry of reduced density matrices, New J. Phys. 18 (2016) 113033.
[59] K. Życzkowski, K.A. Penson, I. Nechita, B. Collins, Generating random density matrices, J. Math. Phys. 52 (2011) 062201.